Construction and Building Materials 79 (2015) 273–282

Contents lists available at ScienceDirect

Construction and Building Materials

journal homepage: www.elsevier.com/locate/conbuildmat

Development of Ultra-High Performance Fibre Reinforced Concrete (UHPFRC): Towards an efficient utilization of binders and fibres

R. Yu [a,*], P. Spiesz [a,b], H.J.H. Brouwers [a]

[a] Department of the Built Environment, Eindhoven University of Technology, Eindhoven, The Netherlands
[b] ENCI HeidelbergCement Benelux, Rotterdam, The Netherlands

HIGHLIGHTS

- A method to efficiently produce UHPFRC is proposed.
- UHPFRC is produced with relatively low binders and fibres content.
- UHPFRC with ternary fibres is designed and produced.
- The effect of hybrid fibres on the flexural toughness of UHPFRC is studied.
- The standards for calculating the UHPFRC toughness are evaluated.

ARTICLE INFO

Article history:
Received 1 September 2014
Received in revised form 5 January 2015
Accepted 6 January 2015

Keywords:
Efficient utilization
Ultra-High Performance Fibre Reinforced Concrete (UHPFRC)
Particle packing model
Hybridization design
Ternary fibres
Flexural toughness

ABSTRACT

This paper presents a method to develop Ultra-High Performance Fibre Reinforced Concrete (UHPFRC). Towards an efficient utilization of binders and fibres in UHPFRC, the modified Andreasen & Andersen particle packing model and the hybridization design of fibres are utilized. Particularly, the UHPFRC with ternary fibres is appropriately designed and tested. The flowability, mechanical properties and flexural toughness of the designed UHPFRC are measured and analyzed. The results show that, based on the optimized particle packing and hybrid macro and micro fibres, it is possible to produce UHPFRC with a relatively low binder amount (about 620 kg/m^3) and low fibre content (Vol. 2%). Moreover, due to the mutual effects between the utilized fibres, the hybrid fibre reinforced UHPFRC shows an improved flowability and better mechanical properties. Nevertheless, the flexural toughness of UHPFRC is dominated by the hooked steel fibres. Due to the specific characteristics of UHPFRC, the JSCE SF-4 standard is found more suitable than ASTM C1018-97 to be used to evaluate the flexural toughness of UHPFRC.

1. Introduction

Ultra-High Performance Fibre-Reinforced Concrete (UHPFRC) is a relatively new construction material, which is a combination of high performance concrete matrix and fibre reinforcement [1–3]. Due to the high binder dosage, low water to binder ratio and relatively high fibre dosage in UHPFRC, it has superior mechanical properties and energy absorption capacity [4–8]. However, as the sustainable development is currently a crucial global issue and various industries are striving in saving energy and lowering environmental impact [8–12], the high material cost, high energy consumption and embedded CO_2 for UHPFRC are the typical disadvantages that restrict its wider application [13–15]. Hence, how to develop UHPFRC efficiently still needs further investigation.

Until now, the most common measures pursued to reduce the economic and environmental disadvantages of UHPFRC are mainly limited to the inclusion of industrial by-products or sometimes waste materials, without sacrificing the superior mechanical properties of UHPFRC [4–6,16–18]. For instance, the granulated blast-furnace slag (GGBS), fly ash (FA) and silica fume (SF) have been used as partial clinker replacements in the production of UHPFRC [16–18]. Furthermore, some waste or recycled materials such as rice husk ash [4,5], recycled glass cullet [6], palm oil fuel ash [19], waste ceramics [20] and waste bottom ash [26] are also utilized to produce UHPFRC. However, in the design of UHPFRC, all of these above mentioned methods did not consider the effect of particle packing on the properties of concrete. In most cases, the recipes of UHPFRC are given directly, without any detailed explanation or theoretical support. Hence, it is questionable whether the concrete matrix is optimal and the binders are used efficiently.

For an appropriate design of mortars and concretes, several mix design tools are in use. Based on the properties of multimodal,

* Corresponding author. Tel.: +31 (0) 40 247 5469; fax: +31 (0) 40 243 8595.
E-mail address: r.yu@tue.nl (R. Yu).

http://dx.doi.org/10.1016/j.conbuildmat.2015.01.050
0950-0618/

discretely sized particles, De Larrard and Sedran [21,22] postulated different approaches to design concrete: the Linear Packing Density Model (LPDM), Solid Suspension Model (SSM) and Compressive Packing Model (CPM). Furthermore, Fennis et al. [23] developed a concrete mix design method based on the concepts of De Larrard and Sedran [21,22]. However, all these design methods are based on the packing fraction of individual solid components (cement, sand, etc.) and their combinations, and therefore it is complicated in practice to include very fine particles in these mix design approaches, as it is difficult to determine the packing fraction of such fine materials or their combinations. Another possibility for the mix design is offered by an integral particle size distribution approach of continuously graded mixes (modified Andreasen & Andersen particle packing model), in which very fine particles can be integrated with considerably lower effort, as detailed in [24]. Additionally, based on the previous experiences and investigations of the authors [25–28], by applying this modified Andreasen & Andersen particle packing model, it is possible to produce a dense and homogeneous skeleton of UHPFRC with a relatively low binder amount (about 650 kg/m^3). Consequently, such an optimized design of the concrete can be a promising approach to produce UHPFRC with an efficient binders use.

Additionally, beside the appropriate design of the concrete matrix, the efficient application of steel fibres is also vital in reducing the materials' cost, energy consumption and embedded CO_2, since the cost of 1% volume content of fibre applied in UHPFRC is generally higher than that of the same volume of matrix [29]. Nevertheless, in many literature positions investigating UHPFRC, the steel fibres are added directly (sometimes with large volumetric amounts, e.g. more than 5% Vol. [30]), without considering the efficiency of the used fibres. Although, an optimal orientation of fibres is beneficial for improving the mechanical properties of concrete, it is very difficult to align all the fibres in the ideal direction [31–35]. Hence, how to find a practical method to efficiently use the steel fibres still needs further studies.

As commonly known, in most cases, the hybrid fibres reinforced concretes have better mechanical properties than the concretes with only a single type of fibres [36–44]. The application of different types of fibres combined in one concrete mixture was firstly proposed by Rossi in 1987 [45], as the so-called multi-modal fibre reinforced concrete (MMFRC). Due to the fact that the short fibres can bridge the microcracks while the long fibres are more efficient in preventing the development of macrocracks, the stress in the hybrid fibres reinforced concrete can be well distributed and its mechanical properties can be improved [42]. From a mechanical point of view, the combination of fibres with different geometry seems to be an optimum solution to increase both the mechanical properties and the ductility [42]. Hence, an appropriate hybridization design of the used steel fibres in the production of UHPFRC can be treated as a potential method to enhance the fibre efficiency. In recent years, the research focusing on the application of hybrid fibres in UHPFRC or influence of hybrid fibres on the UHPFRC properties can also be found in the literature [29,44,46]. However, the research focusing on the application of three different types of steel fibres simultaneously (e.g. ternary fibres blend) in the UHPFRC production is scarce, which may be attributed to the complexity of the design and influence from such ternary fibres blend. Moreover, the available data on the influence of hybrid fibres on the toughness of UHPFRC is very limited. As has been commonly accepted, the toughness properties of UHPFRC are very important when UHPFRC is utilized in elements exposed to large energy release or high impact loading rates [47–51]. Hence, a comprehensive clarification of the relationship between the hybrid fibres and the toughness of UHPFRC is needed.

Based on these premises, the objective of this study is to efficiently develop UHPFRC, and clarify the influence of hybrid or ternary fibres on the properties of UHPFRC. The flowability, mechanical properties and flexural toughness of the designed UHPFRC are measured and analyzed. Based on the obtained results, also the available standards for testing the flexural toughness of concrete are evaluated.

2. Materials and methods

2.1. Materials

The cement used in this study is Ordinary Portland Cement (OPC) CEM I 52.5 R, provided by ENCI HeidelbergCement (The Netherlands). A polycarboxylic ether based superplasticizer is used to adjust the workability of concrete. The limestone powder is used as a filler to replace cement. A commercially available nano-silica in a slurry (AkzoNobel, Sweden) is applied as pozzolanic material. The characteristics of the used nano-silica are shown in Table 1. Two types of sand are used, one is normal sand in the fraction of 0–2 mm and the other one is a microsand in the 0–1 mm size range (Graniet-Import Benelux, The Netherlands). The particle size distributions of the used granular materials are shown in Fig. 1. Additionally, three types of steel fibres are utilized, as shown in Fig. 2: (1) Long straight fibre (LSF), length = 13 mm, diameter = 0.2 mm; (2) Short straight fibre (SSF), length = 6 mm, fibre diameter = 0.16 mm; (3) Hooked fibre (HF) length = 35 mm, diameter = 0.55 mm. The densities of the used materials are shown in Table 2. The oxide compositions of the used cement, limestone powder and nano-silica are presented in Table 3.

2.2. Experimental methodology

2.2.1. Mix design of UHPFRC

In the previous investigations of the authors, it was demonstrated how to produce UHPFRC with a relatively low binder amount [25–28]. Hence, also in this study, the modified Andreasen and Andersen model is utilized to design all the concrete mixtures, which is shown as follows [24,52]:

$$P(D) = \frac{D^q - D_{\min}^q}{D_{\max}^q - D_{\min}^q} \quad (1)$$

where D is the particle size (μm), $P(D)$ is the fraction of the total solids smaller than size D, $D_{\max}$ is the maximum particle size (μm), $D_{\min}$ is the minimum particle size (μm) and q is the distribution modulus.

In the literature, many examples of application of the modified Andreasen and Andersen packing model for the concrete design can be found [53–58]. By using different values of the distribution modulus q, different types of concrete can be designed [55,56,58]. Based on the recommendation of Brouwers [56,58] and Hunger [59], the value of q is fixed at 0.23 in this study, considering that a high content of fines is required in UHPFRC. In the concrete mixture design, the modified Andreasen and Andersen model (Eq. (1)) acts as a target function for the optimization of the composition of mixture of granular materials. The proportions of each individual material in the mix are adjusted until an optimum fit between the composed mix and the target curve is reached, using an optimization algorithm based on the Least Squares Method (LSM), as presented in Eq. (2). When the deviation between the target curve and the composed mix, expressed as the sum of the squares of the residuals (RSS) at defined particle sizes, is minimized, the composition of the concrete is considered optimal [60].

$$\mathrm{RSS} = \frac{\sum_{i=1}^{n}\left(P_{\mathrm{mix}}\left(D_i^{i+1}\right) - P_{\mathrm{tar}}\left(D_i^{i+1}\right)\right)^2}{n} \quad (2)$$

where P_{mix} is the composed mix, the P_{tar} is the target grading calculated from Eq. (1), and n is the number of points (between $D_{\min}$ and $D_{\max}$) used to calculate the deviation.

Table 1
Characteristics of nano-silica.[a]

Type	Slurry
Stabilizing agent	Ammonia
Specific density (g/cm^3)	2.2
pH (at 20 °C)	9.0–10.0
Solid content (% w/w)	20
Viscosity (MPa s)	⩽100
BET (m^2/g)	22.7
PSD by LLS (μm)	0.05–0.3
Mean particle size (μm)	0.12

[a] Data obtained from the supplier.

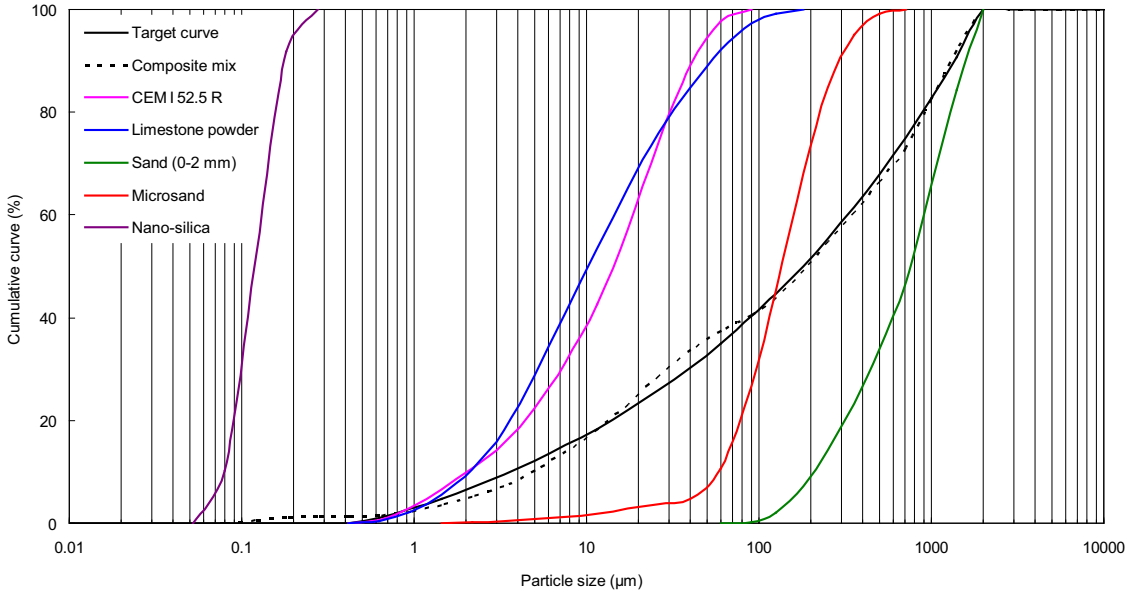

Fig. 1. Particle size distribution of the involved ingredients, the target curve and the resulting integral grading curve of the mixtures.

Fig. 2. Steel fibres used in this study.

Table 2
Information of materials used.

Materials	Type	Specific density (kg/m^3)
Cement	CEM I 52.5 R	3150
Filler	Limestone powder	2710
Fine sand	Microsand	2720
Coarse sand	Sand 0–2	2640
Superplasticizer	Polycarboxylate ether	1050
Pozzolanic material	Nano-silica (nS)	2200
Fibre-1	Long steel fibre (13/0.2)	7800
Fibre-2	Short steel fibre (6/0.16)	7800
Fibre-3	Hooked steel fibre (35/0.55)	7800

As commonly known, the quality of the curve fit is assessed by the coefficient of determination (R^2), since it gives a value for the correlation between the grading of the target curve and the composed mix. Therefore, the coefficient of determination (R^2) is utilized in this study to obtain the optimized mixture given by:

$$R^2 = 1 - \frac{\sum_{i=1}^{n}\left(P_{\mathrm{mix}}\left(D_i^{i+1}\right) - P_{\mathrm{tar}}\left(D_i^{i+1}\right)\right)^2}{\sum_{i=1}^{n}\left(P_{\mathrm{mix}}\left(D_i^{i+1}\right) - \overline{P_{\mathrm{mix}}}\right)^2} \quad (3)$$

where $\overline{P_{\mathrm{mix}}} = \frac{1}{n}\sum_{i=1}^{n} P_{\mathrm{mix}}\left(D_i^{i+1}\right)$, which represents the mean of the entire distribution.

The UHPFRC mixtures developed in this study applying the optimized particle packing model are listed in Table 4. The resulting integral grading curve of the composite mixes is shown in Fig. 1 (R^2 = 0.99). In this study, only about 620 kg/m^3 of binders are used to produce the UHPFRC matrix, which is significantly lower than the amounts reported in the literature [4–12]. In addition, the steel fibres are added into the designed concrete matrix with different hybridizations and proportions (as shown in Table 4). In all the mixtures, the total fibre amount is 2% by the volume of concrete. To analyze the effect of different hybrid fibres on the properties of UHPFRC, two types of hybridization system are designed here: (1) with two types of straight steel fibres (Nos. 2–6 in Table 4); (2) With both hooked steel fibres and two types of straight steel fibres (Nos. 7–10 in Table 4). The mixtures designed with only straight fibres are developed to clarify the effect of the proportions between the long and short fibres on the mechanical properties of UHPFRC, which can further help to design the ternary fibres system.

2.2.2. Mixing procedure

In this study, the concrete matrix is well mixed with steel fibres following the method described in [25]. Before the hybrid fibres are added into the concrete mixture, the fibres are mixed together for 1 min. The mixing is always executed under laboratory conditions with dried and tempered aggregates and powder materials. The room temperature while mixing and testing is constant at around 21 °C.

2.2.3. Flowability of UHPFRC

After mixing, the fresh UHPFRC (Nos. 1–6 in Table 4) is filled in a conical mould in the form of a frustum, as described in EN 1015-3 [61]. Then, the Hägermann cone is lifted straight upwards in order to allow a free flow for the paste without any jolting. Eventually, two diameters (d_1 and d_2) perpendicular to each other are determined. Their mean is recorded as the slump flow value of UHPFRC.

Additionally, considering the effect of hooked long steel fibres, the flowability of fresh mixtures (Nos. 7–10 in Table 4) is tested following EN 12350-8:2010 [62]. The Abrams cone with the internal upper/lower diameter equal to 100/200 mm and

Table 3
Oxide composition of cement, limestone powder and nano-silica.

Substance	Cement (mass %)	Limestone powder (mass %)	Nano-silica (mass %)
CaO	64.60	89.56	0.08
SiO_2	20.08	4.36	98.68
Al_2O_3	4.98	1.00	0.37
Fe_2O_3	3.24	1.60	–
K_2O	0.53	0.34	0.35
Na_2O	0.27	0.21	0.32
SO_3	3.13	–	–
MgO	1.98	1.01	–
TiO_2	0.30	0.06	0.01
Mn_3O_4	0.10	1.605	–
P_2O_5	0.74	0.241	0.15
Cl^-	0.05	–	0.04

height equal to 300 mm is utilized without any jolting. Two diameters (d_1 and d_2) perpendicular to each other are recorded and their mean is recorded as the slump flow value of UHPFRC.

2.2.4. Mechanical properties of UHPFRC

After preforming the flowability test, the fresh UHPFRC mixtures (Nos. 1–6 in Table 4) is cast in moulds with the size of 40 mm × 40 mm × 160 mm. The prisms are demoulded approximately 24 h after casting and subsequently cured in water at about 21 °C. After curing for 7 and 28 days, the compressive and flexural strengths of the prism specimens are tested according to the EN 196-1 [63]. At least three specimens are tested for each batch.

Additionally, considering the restriction of the hooked fibres on the size of the mould, the fresh UHPFRC mixtures (Nos. 7–10 in Table 4) are cast in moulds with the size of 100 mm × 100 mm × 500 mm and 100 mm × 100 mm × 100 mm. The beams and cubes are demoulded approximately 24 h after casting and subsequently cured in water at about 21 °C. After curing for 28 days, the compressive strengths of the cubes are determined according to EN 12390-3 [64], and the beams are subjected to the 4-point bending test as described in EN 12390-5 [65]. For the 4-point bending test, the span between the two supported points at the bottom is 400 mm. To obtain flexural load over the middle deflection curve, a Linear Variable Differential Transformer (LVDT) mounted on the surface of the tested samples is utilized to record the mid-deflection. During the test, the set-up is running in a displacement control mode, which is set at 0.1 mm/min. The test device and a scheme of the sample during the test are illustrated in Fig. 3. Before the test, the calibration of the LVDT is done.

2.2.5. Flexural toughness of UHPFRC

According to the available literature, two standards are mainly used to evaluate the flexural toughness of fibre reinforced concrete, which are ASTM C1018-97 [66] and JSCE SF-4 [67]. In this study, both these standards are utilized to calculate the flexural toughness of UHPFRC.

In ASTM C1018-97, the flexural toughness is calculated at four specified deflections (δ, 3δ, 5.5δ and 10.5δ). The δ represents the deflection when the first crack appears, as presented in Fig. 4. The flexural toughness is calculated at the deflection δ, which is considered the elastic or pre-peak flexural toughness (first-crack flexural toughness), while the other three (3δ, 5.5δ and 10.5δ) are considered as the post-peak flexural toughnesses. Furthermore, the flexural toughness indices I_5, I_{10} and I_{20} are also defined, which are the ratios between the post-peak flexural toughness and the pre-peak (elastic) flexural toughness. Based on Fig. 4, the flexural toughness indices can be calculated as:

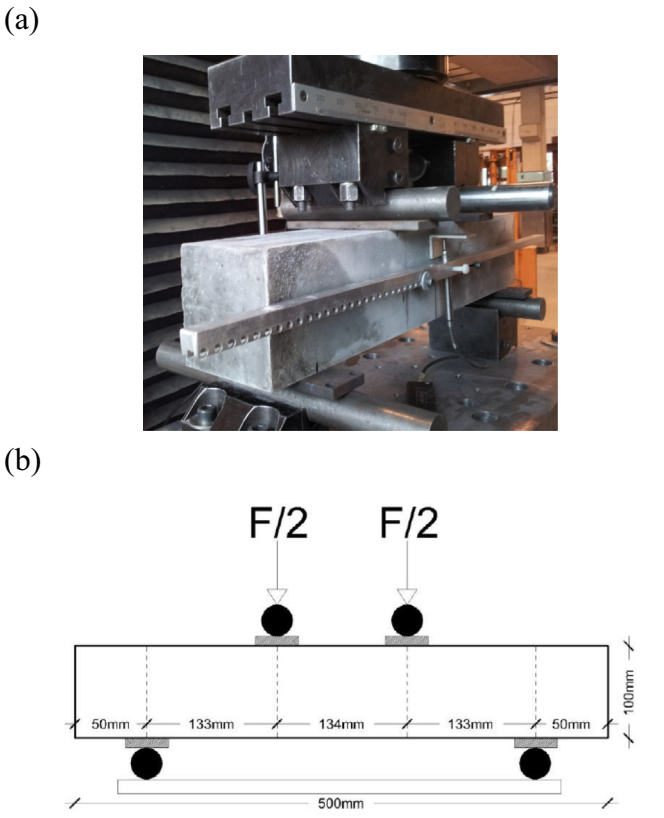

Fig. 3. Employed 4-point bending test device (a) and schema a sample during the test (b).

$$I_5 = \frac{\text{Area OACD}}{\text{Area OAB}} \tag{4}$$

$$I_{10} = \frac{\text{Area OAEF}}{\text{Area OAB}} \tag{5}$$

$$I_{20} = \frac{\text{Area OAGH}}{\text{Area OAB}} \tag{6}$$

Differently from the ASTM C1018-97, the JSCE SF-4 defines the area under the load–deflection plot up to a deflection of span/150 as the flexural toughness. From this measurement, a flexural toughness factor (*TF*) can be calculated as follows:

$$TF = \frac{A_{(L/150)} \cdot L}{(L/150)BH^2} \tag{7}$$

where *TF* represents the flexural toughness factor, *L* is the span, $A_{(L/150)}$ is the flexural toughness at the deflection (*L*/150) (calculated in this study using Matlab), *B* is the specimen's width and *H* is the specimen's height.

Table 4
Recipes of the developed UHPFRC.

No.	C (kg/m^3)	LP (kg/m^3)	M-S (kg/m^3)	N-S (kg/m^3)	nS (kg/m^3)	W (kg/m^3)	SP (kg/m^3)	LSF (Vol. %)	SSF (Vol. %)	HF (Vol. %)
1	594.2	265.3	221.1	1061.2	24.8	176.9	44.2	0	0	0
2	594.2	265.3	221.1	1061.2	24.8	176.9	44.2	2.0	0	0
3	594.2	265.3	221.1	1061.2	24.8	176.9	44.2	1.5	0.5	0
4	594.2	265.3	221.1	1061.2	24.8	176.9	44.2	1.0	1.0	0
5	594.2	265.3	221.1	1061.2	24.8	176.9	44.2	0.5	1.5	0
6	594.2	265.3	221.1	1061.2	24.8	176.9	44.2	0	2.0	0
7	594.2	265.3	221.1	1061.2	24.8	176.9	44.2	0	0	2
8	594.2	265.3	221.1	1061.2	24.8	176.9	44.2	0.125	0.375	1.5
9	594.2	265.3	221.1	1061.2	24.8	176.9	44.2	0.5	0	1.5
10	594.2	265.3	221.1	1061.2	24.8	176.9	44.2	0	0.5	1.5

C: cement, LP: limestone powder, M-S: microsand, N-S: normal sand, nS: nano-silica, W: water, SP: superplasticizer, LSF: long straight fibre, SSF: short straight fibre, HF: hooked fibre.

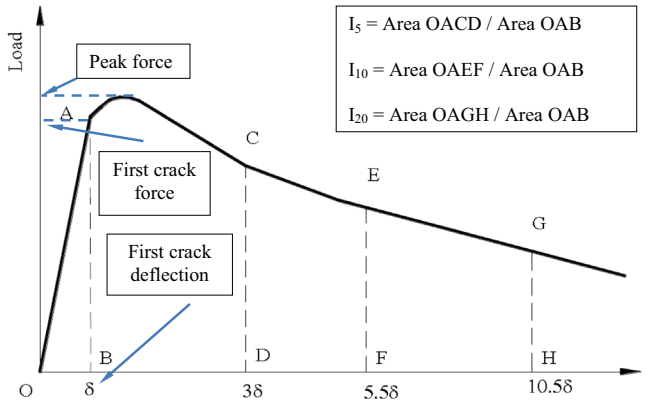

Fig. 4. Typical load–deflection curve for fibre reinforced concrete and fracture toughness indices based on ASTM C 1018.

3. Experimental results and discussion

3.1. Flowability of UHPFRC

The slump flow of the fresh UHPFRC mixtures with only straight fibres is shown in Fig. 5. The data illustrates the variation of the slump flow of UHPFRC with different short straight fibre (SSF) and long straight fibre (LSF) amounts. SSF-0, SSF-0.5, SSF-1.0, SSF-1.5 and SSF-2.0 represent the mixtures from Nos. 2 to 6, respectively (see Table 4). It can be clearly seen that the slump flows of the designed UHPFRC are all larger than 25 cm, and fluctuate around 29 cm, which can treated as self-compacting mortar, according to the European Guidelines for Self-Compacting Concrete [68] and the recommendation presented in [59]. Moreover, it is important to notice that with an increase of the SSF amount (simultaneous decrease of LSF) in the fresh concrete mixtures, the slump flow ability of UHPFRC firstly increases, and then sharply decreases when only the short straight fibres are present. For example, when there are only long straight fibres (LSFs) in the concrete mixture, the slump flow is 28.8 cm, which slightly increases to around 30.0 cm when 0.5% Vol. LSF and 1.5% Vol. SSF are added. However, when all the LSF are replaced by SSF, the flowability of the UHPFRC reduces to about 28.3 cm, which is even smaller than that of mixture with only LSF.

Fig. 6 illustrates the slump flow of UHPFRC with hooked fibres (HF). The data presents the variation of slump flow of UHPFRC with different fibres hybridization. The HF, HF + LSF + SSF, HF + LSF and HF + SSF represent the mixtures from Nos. 7 to 10, respectively (see Table 4). As can be noticed, the slump flow of all the designed UHPFRC with HF fluctuates around 85 cm, which is much more than that shown in Fig. 5, because different cones are used in these two flowability tests. The mixture with HF and SSF has the highest slump flow value (88.5 cm), which is followed by the one with ternary fibres. The UHPFRC with only HF shows the smallest slump flow value, around 83.5 cm. According to the European Guidelines for Self-Compacting Concrete [68], the slump flow of concrete is divided into three classes: (1) SF 1: 55–65 cm; (2) SF 2: 66–75 cm; (3) SF 3: 76–85 cm. The slump flows of the designed UHPFRCs with HF are all in the SF 3class, which implies that it is possible to produce a UHPFRC with a high flowability. Particularly, when the SSF is utilized, the flowability of UHPFRC can be further improved.

As commonly known, the effect of steel fibres on the flowability of concrete is mainly due to four reasons: (1) The shape of the fibres is much more elongated compared with aggregates and the surface area at the same volume is higher, which can increase the cohesive forces between the fibres and the matrix [52]; (2) Stiff fibres change the structure of the granular skeleton, and also push apart particles that are relatively large compared with the fibre length [52]; (3) Steel fibres are often deformed (e.g. have hooked ends or are wave-shaped) to improve the anchorage between the fibre and the surrounding matrix [52]; (4) Mutual effects between the hybrid fibres [28]. Moreover, it is known that different flow velocities affect the fibres and may cause them to rotate in such a way that the fibres reorient perpendicularly to the flow direction. Hence, for the fresh concrete with a single fibre type, the fibres orientation tends to be perpendicular to the flow direction in the fountain flowing mode, which can generate the largest resistance force and reduce the slump flow of the fresh concrete [69]. Nevertheless, when hybrid fibres are added into the concrete, the fountain flowing mode may be disturbed. Due to the difference in geometry, the rotation of fibres can be restricted by each other, which causes that the resistance force in the fountain flow can be reduced and the slump flow value of the concrete mixture could be higher. Hence, as observed in this study, the hybrid fibre reinforced concretes have a higher slump flow ability than the mixtures with only single type of fibres, similarly to the observation reported in [28].

3.2. Mechanical properties of UHPFRC

3.2.1. Mechanical properties of UHPFRC with only straight steel fibres

The flexural strengths of the designed UHPFRC with only straight steel fibres are shown in Fig. 7(a). The "Reference" represents the mixture without fibres (mixture No. 1 in Table 4). It is clear that the addition of fibres significantly improves the mechanical properties of concrete. However, the improvement depends on different fibres hybridization. As can be seen, the flexural strengths of the

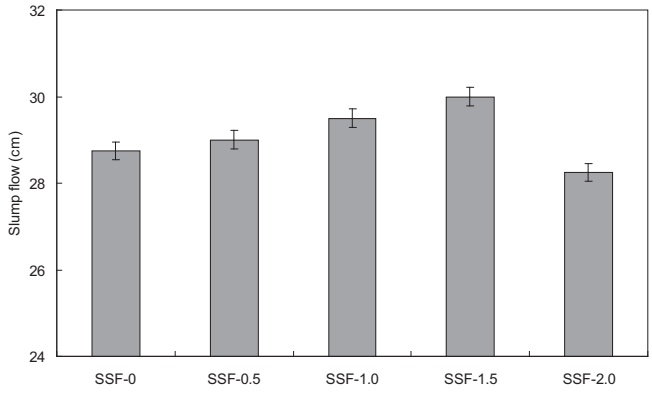

Fig. 5. Variation of the slump flow (using the Hägermann cone) of the developed UHPFRC with only straight steel fibres (SSF-0, SSF-0.5, SSF-1.0, SSF-1.5 and SSF-2.0 represent the mixtures shown in Table 4, from Nos. 2 to 6, respectively).

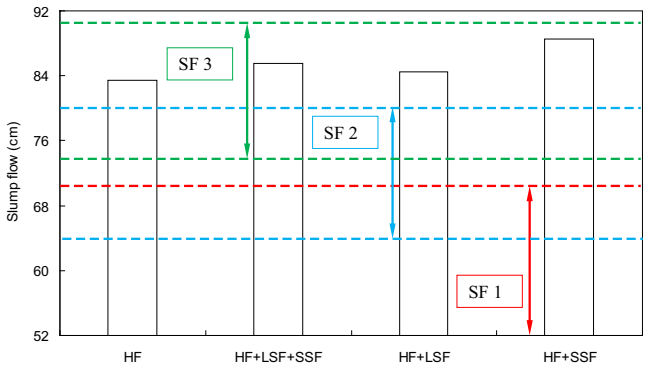

Fig. 6. Slump flow of the developed UHPFRC with hooked fibres (HF, HF + LSF + SSF, HF + LSF and HF + SSF represent the mixtures from Nos. 7 to 10, respectively.

concrete with LSF (1.5% Vol.) and SSF (0.5% Vol.) at 7 and 28 days are always the highest, which are 24.3 MPa and 30.9 MPa, respectively. When only SSF is utilized (2% Vol.), the flexural strengths at 7 and 28 days reduce to around 18.4 MPa and 21.5 MPa, respectively. This can be explained by the following two reasons: (1) SSF can efficiently bridge microcracks, while LSF is more efficient in resisting the development of macrocracks. Hence, when the microcracks are just generated in the concrete specimen, the SSF can effectively bridge them. As the microcracks grow and merge into larger macrocracks, LSF become more active in crack bridging. In this way, the flexural strength of UHPFRC can be improved; (2) LSF are always well oriented between the two imaginary borders, and these borders may also be the walls of the moulds. With such positions, LSF form a kind of a barrier for SSF, and limit their space for rotation. The SSF will therefore be somewhat better oriented when combined together with LSF, than on their own [42]. Hence, more fibres distribute in the direction perpendicular to the load direction in the flexural test, thus the mechanical properties can be significantly improved.

Fig. 7(b) presents the compressive strength of UHPFRC with only straight steel fibres. As can be observed, compared to the reference sample, the additional steel fibres can also significantly increase the compressive strength of UHPFRC. Moreover, the mixture with LSF (1.5% Vol.) and SSF (0.5% Vol.) shows the highest compressive strengths, which are 117.1 MPa and 141.5 MPa after curing for 7 and 28 days, respectively. This should also be attributed to the combined effect of hybrid fibres in restricting the cracks development. Moreover, the compressive strength results demonstrate that, based on the modified Andreasen & Andersen particle packing model and appropriate fibre hybridization design, it is possible to produce UHPFRC with a relatively low binder and fibre content.

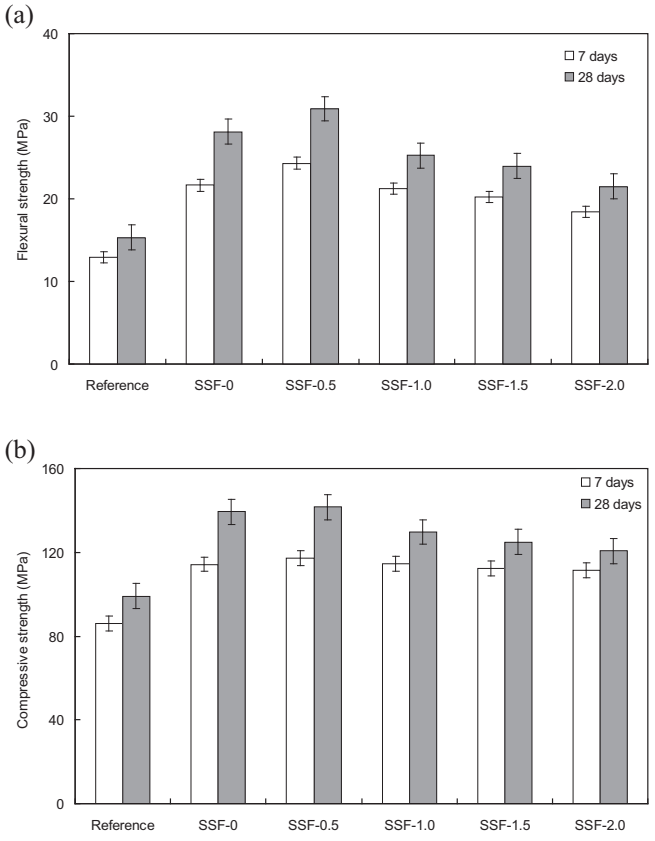

Fig. 7. Flexural (a) and compressive (b) strength of the developed UHPFRC with only straight steel fibres (Reference: UHPFRC without fibres).

3.2.2. Mechanical properties of UHPFRC with hooked steel fibres

Considering that the hooked fibre (HF) is one of the most commonly used steel fibre type for the production of steel fibre reinforced concrete, the HF (macro-fibre) is included in the production of UHPFRC, as shown in Table 4, Nos. 7–10. Due to the fact that the designed UHPFRC mixture with LSF (1.5% Vol.) and SSF (0.5% Vol.) at 7 and 28 days shows the best mechanical properties (as shown in Fig. 7), the designed volumetric ratio of HF/LSF or HF/SSF are all chosen as 3:1. In addition, in the mixture with ternary hybrid fibres, the volumetric ratio of HF/LSF/SSF is fixed at 12:3:1 (thus, the volumetric ratio of hooked fibres (long) to straight fibres (short) is still 3:1).

Fig. 8 illustrates the compressive strength of UHPFRC with hooked steel fibres (HF). It can be found that the 28 days compressive strength of all the designed mixtures fluctuates around 135 MPa, and the difference between the mixtures with HF is relatively small. For instance, the mixture with HF and SSF shows the highest compressive strength at 28 days (136.5 MPa), while that the reference mixture (with only HF) is the lowest – 129.2 MPa. Moreover, in the mixtures HF + LSF + SSF, HF + LSF and HF + SSF, the HF amount is the same (1.5% Vol.), and their compressive strengths follow the order: HF + SSF > HF + LSF + SSF > HF + LSF. Hence, it can be concluded that: (1) when the total fibre amount is the same, the mixture with hybrid fibres shows a higher compressive strength than the one with HF only; (2) In the hybrid fibres system, when the total fibre and the HF amounts are the same, the SSF is more efficient in improving the compressive strength than the LSF. These phenomena could be also attributed to the combined effect of hybrid fibres in restricting the cracks development. The homogeneity of the tested sample is very important to improve its compressive strength. As can be easily understood, with the same volumetric amount, the SSF has the largest fibre number compared to the other used fibres. Hence, in this study, the UHPFRC mixture with HF + SSF is more homogeneous, so it compressive strength can be larger compared to the sample with HF + LSF or HF only.

Fig. 9 presents the 4-point bending test results of UHPFRC with HF. The load/mid-deflection curves can be mainly divided into three parts: elastic section, strain hardening section and strain softening section, as shown in Fig. 10. From the beginning of the test until the moment when the first crack appears, the linear section part of the curve can be observed. Due to the fact that the tested UHPFRC is very stiff, very small mid-deflections of the samples can be measured. In this study, the first crack deflection for all the samples fluctuates around 0.01 mm, and the first crack forces follow the order: HF + LSF + SSF (30.9 kN) > HF + SSF (30.3 kN) > HF + LSF (30.1 kN) > HF (28.1 kN). It can be observed that the first crack forces of the mixtures with hybrid fibres are similar to each other, and are obviously larger than the one with HF only. After the first

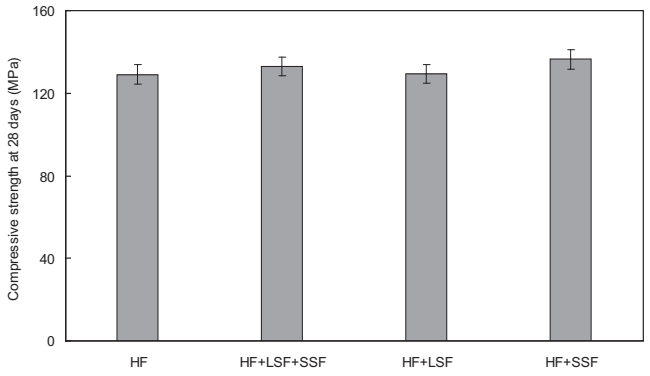

Fig. 8. Compressive strength test results of the developed UHPFRC with hooked fibres (HF, HF + LSF + SSF, HF + LSF and HF + SSF represent the mixtures from Nos. 7 to 10, respectively).

crack appears, the strain hardening section starts, and a number of small cracks generates in the tested beam, as shown in Fig. 9. In this process, the fibres in concrete will mainly endure the load and limit the growth of the generated cracks, until the peak force appears. In this study, the peak forces for the tested UHPFRC follow the order: HF + LSF + SSF (43.1 kN) > HF + SSF (39.9 kN) > HF + LSF (38.2 kN) > HF (34.8 kN), and this trend is similar to that of the first crack force. When the fibres in concrete cannot restrain the further growth of the small cracks, the fibres will be pulled out and the endurable force of the test beam will decrease, which reflects the initiation of the strain softening section. Nevertheless, due to the different characteristics of the fibres and the binding force between the fibres and concrete matrix, the strain softening behaviour of reinforced concrete can be very different. In this study, it is important to notice that the endurable force of the mixtures with SSF (e.g. HF + LSF + SSF and HF + LSF) sharply decreases after reaching the peak force, while for concrete with only HF or HF + LSF a relatively slow decreasing trends are observed. The decreasing rates of the residual load of the tested UHPFRCs follow the order: HF < HF + LSF < HF + LSF + SSF < HF + SSF, which also implies that the addition of SFF (instead of longer fibres) may significantly reduce the flexural toughness of UHPFRC. This phenomenon can be attributed to the following reasons: (1) during the 4-point bending test, the hybrid fibres can well disperse the loading force. For instance, the straight fibres can well bridge the microcracks, while the long hooked fibres are more efficient in resisting the macrocracks development. Hence, when ternary fibres are used in UHPFRC, the cracks generated at different length-scales can be better bridged compared to the mixture with only one or two types of fibres, which causes that the endurable force can be simultaneously larger; (2) Due to the multiple effects among different fibres, more fibres in the ternary fibres reinforced mixture distribute in the direction perpendicular to the force direction during the 4-point bending test, which can further improve the first crack force and peak force; (3) Although SSF works well in restraining the growth of microcracks, it is less efficient during the strain softening process, which should be attributed to its geometry. Due to the relatively short length and lower binding force with the concrete matrix, many SSF can be pulled out after reaching the peak force, and the load endurable capacity of the tested beam sharply decreases. In contrary to the characteristic of SSF, HF shows a greater ability in restraining the development of macrocracks. As commonly known, the hooks at the ends of HF can improve the coupling force between the fibres and concrete matrix, which causes that a higher force is needed to pull this fibre type out (compared to SSF). Hence, during the strain softening process, HF can still bridge the macrocracks, and the endurable force with only HF can slowly decrease with an increase of the mid-deflection.

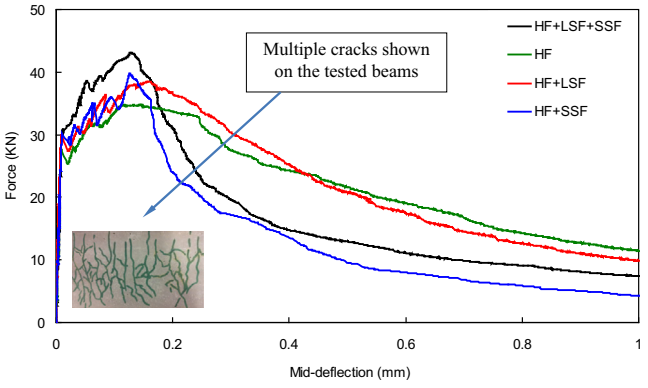

Fig. 9. 4-Point bending test results of the developed UHPFRC beam with hooked fibres (HF, HF + LSF + SSF, HF + LSF and HF + SSF represent the mixtures from Nos. 7 to 10, respectively).

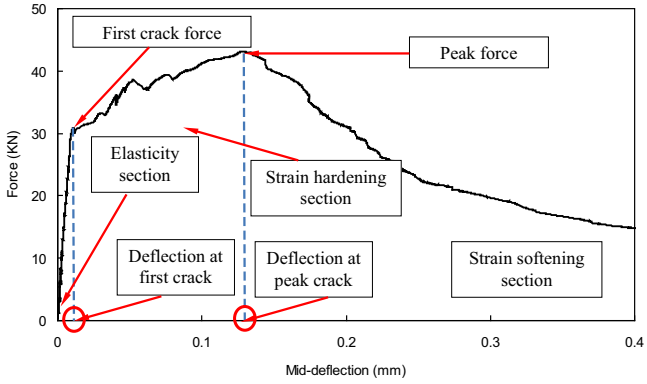

Fig. 10. Characteristic parameters of UHPFRC beam subjected to 4-point bending test.

3.3. Flexural toughness of UHPFRC

To evaluate the effect of different fibres on the flexural toughness of UHPFRC, the procedures described in ASTM C1018-97 [66] and JSCE SF-4 [67] are employed for the flexural toughness determination, as described in Section 2.2.5.

3.3.1. Flexural toughness calculated based on ASTM C1018-97

Fig. 11 shows the flexural toughness of UHPFRC calculated based on ASTM C1018-97. It can be noticed that the first crack flexural toughnesses of the tested UHPFRC are very small and similar to each other, and fluctuate around 0.2 N m. After that, with a deflection increase, a difference between the post crack flexural toughnesses of UHPFRC can be observed. Especially at the deflection of 10.5 δ, the mixture with ternary fibres has the largest post crack flexural toughness (4.1 N m), which is followed by the HF + SSF (3.3 N m), HF + LSF (3.2 N m) and HF (3.1 N m), respectively. Hence, based on the ASTM C1018-97, the flexural toughness of the mixture with ternary fibres is the highest, while the flexural toughness of the mixture with only HF is the smallest. In addition, the flexural toughness indices of all the mixtures are calculated based on ASTM C1018-97, and are presented in Fig. 12. It can be noticed that the I_5 for all the mixtures are similar to each other, which is similar to the first crack flexural toughness shown in Fig. 11. Moreover, the indices I_{10} and I_{20} show that the tested concretes with different fibres follow the order: HF > HF + LSF + SSF > HF + LSF > HF + SSF. Hence, it can be summarized that the concrete mixture with only HF has the largest flexural toughness, which is closely followed by the mixture with ternary fibres. However, it is important to notice that the calculated flexural toughness and flexural toughness indices are contradicting, which implies that the standard ASTM C1018-97 is not very suitable to evaluate the flexural toughness of UHPFRC (see Fig. 13).

3.3.2. Flexural toughness calculated based on JSCE SF-4

To clarify the conflicting results of flexural toughness based on ASTM C1018-97, the JSCE SF-4 is employed to further evaluate the flexural toughness of UHPFRC. The calculated flexural toughness and flexural toughness factors of UHPFRC based on JSCE SF-4 are shown in Fig. 13. It is obvious that the calculated flexural toughnesses presented in Fig. 13 are all in the range from 25 to 35 N m, and are much larger than those calculated based on ASTM C1018-97 (shown in Fig. 11). In addition, according to the literature, the flexural toughness of UHPFRC calculated based on JSCE SF-4 is similar to the results of other fibre reinforced concretes, as shown in [70,71]. Moreover, the calculated flexural toughnesses and flexural toughness factors shown in Fig. 13 follow the same order:

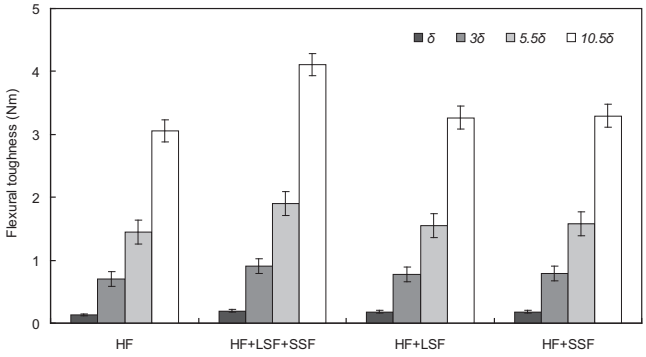

Fig. 11. Calculated flexural toughness of the developed UHPFRC based on ASTM C1018-97 (HF, HF + LSF + SSF, HF + LSF and HF + SSF represent the mixtures from Nos. 7 to 10, respectively).

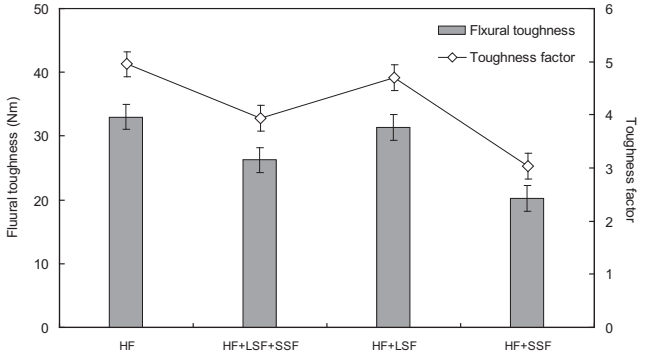

Fig. 13. Calculated flexural toughness and flexural toughness factor of the developed UHPFRC based on JSCE SF-4 (HF, HF + LSF + SSF, HF + LSF and HF + SSF represent the mixtures from Nos. 7 to 10, respectively).

HF > HF + LSF > HF + LSF + SSF > HF + SSF, which is in line with the obtained 4-point bending test results (Fig. 9). Hence, it is demonstrated that the HF can significantly increase the flexural toughness of UHPFRC, while that the additional SSF is less effective in improving the flexural toughness of UHPFRC.

3.3.3. Comparison of ASTM C1018-97 and JSCE SF-4

In this study, it can be noticed that the flexural toughness calculated based on ASTM C1018-97 and JSCE SF-4 show very different results. Hence, it makes sense to assess the employed standards and clarify which one is more suitable to be used to calculate the flexural toughness of UHPFRC. In the literature it can be noticed that these two standards are the most widely used standards to determine the flexural toughness of concrete or fibre reinforced concrete. Some comparisons and evaluations between these standards can be easily found. For instance, Nataraja [70] stated that the characterization of flexural toughness based on the JSCE SF-4 approach was very simple and was independent of the type of the deflection measuring technique. No sophisticated instrumentation was required to determine the flexural toughness factor. Moreover, Sukontasukkul [71] found that a single value flexural toughness determined using JSCE SF-4 method can easily reflect the flexural toughness property of steel fibre reinforced concretes (SFRC). However, in the case of polypropylene fibre reinforced concrete (PFRC), JSCE SF-4 does not seem to be sufficient to reflect the true flexural toughness. On the other hand, the flexural toughness calculated by ASTM C1018-97 at different deflections seems to work well in terms of capturing and reflecting the true flexural toughness properties of both SFRC and PFRC [71].

However, in this study, after comparing the obtained 4-point bending test results and the calculated flexural toughness, it can be found that the ASTM C1018-97 cannot correctly reflect the flexural toughness property of the tested UHPFRC, which is not in line with the conclusion of Sukontasukkul [71]. This should be attributed to the difference of the first crack deflection between the normal strength concrete and UHPFRC. As can be seen, the flexural toughness described in ASTM C1018-97 largely depends on the value of the deflection of the first crack (e.g. δ, 3δ, 5.5δ and 10.5δ). In the 4-point bending test of UHPFRC, due to the fact that UHPFRC is very stiff, its deflection at the first crack appearance is much smaller than for the normal fibre reinforced concrete. In this study, the δ of all the tested mixtures fluctuates around 0.01 mm, which causes that the calculated 3δ, 5.5δ and 10.5δ are also relatively small. Hence, in the calculation of the flexural toughness following ASTM C 1018, only small part of the area under the load–deflection curve is considered. As shown in Fig. 9, the deflection of 10.5δ (around 0.11 mm) is still in the strain hardening section. Hence, the flexural toughness calculated based on ASTM C1018-97 cannot truly represent the flexural toughness property of UHPFRC. In contrary, in the standard JSCE SF-4, the area under the load–deflection plot up to a deflection of span/150 (about 2.67 mm in this study) is calculated, which guarantees that the section of elasticity, strain hardening and strain softening are all taken into account in the flexural toughness calculation. Consequently, it can be summarized that the JSCE SF-4 is more suitable to evaluate the flexural toughness property of UHPFRC than ASTM C1018-97.

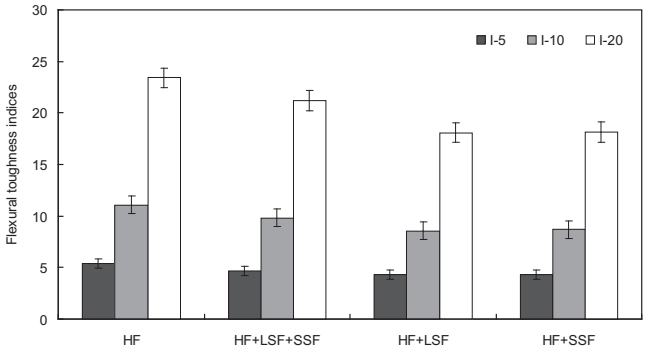

Fig. 12. Calculated flexural toughness indices of the developed UHPFRC based on ASTM C1018-97 (HF, HF + LSF + SSF, HF + LSF and HF + SSF represent the mixtures from Nos. 7 to 10, respectively).

4. Conclusions

This paper presents a method to efficiently develop Ultra-High Performance Fibre Reinforced Concrete (UHPFRC). Towards an efficient application of binders and fibres in UHPFRC, the modified Andreasen & Andersen particle packing model and the hybridization design of fibres are utilized. Particularly, the ternary fibres reinforced UHPFRC is appropriately designed, produced, tested and analyzed. From the results obtained in this paper the following conclusions can be drawn:

- Using the Andreasen & Andersen particle packing model and optimized fibres hybridization, it is possible to produce a stiff UHPFRC with relatively low binder amount (about 620 kg/m^3) and low fibre amount (Vol. 2%), which can make the concrete more sustainable and cost effective.
- Both the straight and the hooked fibres can be used to produce UHPFRC with relatively good flowability. Moreover, with the same steel fibre amount, the hybrid fibre reinforced concrete shows better workability than the one with a single type of fibres. This may be attributed to the fact that the long fibres can be treated as imaginary borders to the short fibres, so that they can

relatively well resist the rotation of the short fibres and reduce the resistance force in the fountain flowing. Furthermore, the short fibres can also conversely restrict the rotation of the long fibres.

- The UHPFRC mixtures with hybrid fibres have higher strengths than those with a single type of fibres. The macro-fibres (hooked steel fibres) can also be utilized to produce UHPFRC, with good mechanical properties. The addition of short straight fibres (SSFs) can significantly improve the homogeneity of the concrete mixture and simultaneously enhance its compressive strength, while the ternary hybrid fibres are beneficial in increasing the peak force of UHPFRC in the 4-point bending test. Hence, based on different requirements on the mechanical properties of UHPFRC, various hybridization designs of the fibres can be executed, which can significantly improve the fibre efficiency.
- The flexural toughness of UHPFRC is evaluated following the most commonly used standards (ASTM C1018-97 and JSCE SF-4). The results show that, with the same fibre amount, the hooked fibres (HF) can significantly increase the flexural toughness of UHPFRC, while that the additional short straight fibres (SSFs) are less effective in improving the flexural toughness of UHPFRC. Moreover, due to the specific characteristics of UHPFRC, it is found that the JSCE SF-4 guideline is more suitable for UHPFRC flexural toughness evaluation than ASTM C1018-97.

Symbols

$A_{(L/150)}$	calculated flexural toughness at the deflection (L/150) (N m)
B	width of the test specimen (mm)
d_1	diameter of the spread of concrete mixtures (mm)
d_2	diameter of the spread of concrete mixtures (perpendicular to d_1) (mm)
D	particle size (μm)
D_{max}	maximum particle size (μm)
D_{min}	minimum particle size (μm)
H	height of the test specimen (mm)
I_5	flexural toughness index
I_{10}	flexural toughness index
I_{20}	flexural toughness index
L	span during the 4-point bending test (mm)
P_{mix}	composed mix
P_{tar}	target curve
$P(D)$	a fraction of the total solids being smaller than size D
q	distribution modulus
RSS	sum of the squares of the residuals
δ	deflection when the first crack appears (mm)

Abbreviations

ASTM	American Society for Testing and Materials
CPM	Compressive Packing Model
HF	Hooked fibre
JSCE	Japan Society of Civil Engineers
LPDM	Linear Packing Density Model
LSF	Long straight fibre
LSM	Least Squares Method
OPC	Ordinary Portland Cement
SCUHPFRC	Self-Compacting Ultra-High Performance Fibre Reinforced Concrete
SSF	Short straight fibre
SSM	Solid Suspension Model
TF	Flexural toughness factor
UHPFRC	Ultra-High Performance Fibre Reinforced Concrete

Acknowledgements

The authors wish to express their gratitude to MSc. Nikos Kanavas for assisting the experimental work and contributing to Figs. 2 and 4. Moreover, the appreciation goes to the following sponsors of the Building Materials research group at TU Eindhoven: Graniet-Import Benelux, Kijlstra Betonmortel, Struyk Verwo, Attero, ENCI, Provincie Overijssel, Rijkswaterstaat Zee en Delta - District Noord, Van Gansewinkel Minerals, BTE, V.d. Bosch Beton, Selor, Twee "R" Recycling, GMB, Schenk Concrete Consultancy, Geochem Research, Icopal, BN International, Eltomation, Knauf Gips, Hess ACC Systems, Kronos, Joma, CRH Europe Sustainable Concrete Centre, Cement&BetonCentrum, Heros and Inashco (in chronological order of joining).

References

[1] Richard P, Cheyrezy M. Composition of reactive powder concretes. Cem Concr Res 1995;25(7):1501–11.
[2] Aldahdooh MAA, Bunnori NM, Johari MAM. Evaluation of ultra-high-performance-fiber reinforced concrete binder content using the response surface method. Mater Des 2013;52:957–65.
[3] Ghafari E, Costa H, Júlio E, Portugal A, Durães L. The effect of nanosilica addition on flowability, strength and transport properties of ultra-high performance concrete. Mater Des 2014;59:1–9.
[4] Tuan NV, Ye G, Breugel K, Copuroglu O. Hydration and microstructure of ultra-high performance concrete incorporating rice husk ash. Cem Concr Res 2011;41:1104–11.
[5] Tuan NV, Ye G, Breugel K, Fraaij ALA, Dai BD. The study of using rice husk ash to produce ultra-high performance concrete. Constr Build Mater 2011;25:2030–5.
[6] Yang SL, Millard SG, Soutsos MN, Barnett SJ, Le TT. Influence of aggregate and curing regime on the mechanical properties of ultra-high performance fibre reinforced concrete (UHPFRC). Constr Build Mater 2009;23:2291–8.
[7] Toledo Filho RD, Koenders EAB, Formagini S, Fairbairn EMR. Performance assessment of ultra high performance fiber reinforced cementitious composites in view of sustainability. Mater Des 2012;36:880–8.
[8] Yu R, Shui ZH. Influence of agglomeration of a recycled cement additive on the hydration and microstructure development of cement based materials. Constr Build Mater 2013;49:841–51.
[9] Silvestre R, Medel E, García A, Navas J. Utilizing recycled ceramic aggregates obtained from tile industry in the design of open graded wearing course on both laboratory and in situ basis. Mater Des 2013;50:471–8.
[10] Shui ZH, Yu R, Dong J. Activation of fly ash with dehydrated cement past. ACI Mater J 2011;108(2):204–8.
[11] Ozger OB, Girardi F, Giannuzzi GM, Salomoni VA, Majorana CE, Fambri L, et al. Effect of nylon fibres on mechanical and thermal properties of hardened concrete for energy storage systems. Mater Des 2013;51:989–97.
[12] Yu R, Shui ZH. Efficient reuse of the recycled construction waste cementitious materials. J Clean Prod 2014;78:202–7.
[13] UNSTATS. Greenhouse gas emissions by sector (absolute values). United Nation Statistical Division. Springer; 2010.
[14] Friedlingstein P, Houghton RA, Marland G, Hackler J, Boden TA, Conway TJ, et al. Uptake on CO_2 emissions. Nat Geosci 2010;3:811–2.
[15] Habert G, Denarié E, Šajna A, Rossi P. Lowering the global warming impact of bridge rehabilitations by using Ultra High Performance Fibre Reinforced Concretes. Cem Concr Compos 2013;38:1–11.
[16] Yu R, Spiesz P, Brouwers HJH. Development of an eco-friendly Ultra-High Performance Concrete (UHPC) with efficient cement and mineral admixtures uses. Cem Concr Compos 2015;55:383–94.
[17] Hassan AMT, Jones SW, Mahmud GH. Experimental test methods to determine the uniaxial tensile and compressive behaviour of Ultra-High Performance Fibre Reinforced Concrete (UHPFRC). Constr Build Mater 2012;37:874–82.
[18] Tayeh BA, Abu Bakar BH, Megat Johari MA, Voo YL. Mechanical and permeability properties of the interface between normal concrete substrate and ultra-high performance fibre concrete overlay. Constr Build Mater 2012;36:538–48.

[19] Aldahdooh MAA, Muhamad Bunnori N, Megat Johari MA. Development of green Ultra-High Performance Fiber Reinforced Concrete containing ultrafine palm oil fuel ash. Constr Build Mater 2013;48:379–89.
[20] Vejmelková E, Keppert M, Rovnaníková P, Ondráček M, Keršner Z, Černy R. Properties of high performance concrete containing fine-ground ceramics as supplementary cementitious material. Constr Build Mater 2012;34:55–61.
[21] De Larrard F, Sedran T. Optimization of ultra-high-performance concrete by the use of a packing model. Cem Concr Res 1994;24:997–1009.
[22] De Larrard F, Sedran T. Mixture-proportioning of high-performance concrete. Cem Concr Res 2002;32:1699–704.
[23] Fennis SAAM, Walraven JC, den Uijl JA. The use of particle packing models to design ecological concrete. Heron 2009;54:185–204.
[24] Andreasen AHM, Andersen J. Über die Beziehungen zwischen Kornabstufungen und Zwischenraum in Produkten aus losen Körnern (mit einigen Experimenten). Kolloid-Zeitschrift 1930;50:217–28 (In German).
[25] Yu R, Spiesz P, Brouwers HJH. Mix design and properties assessment of Ultra-High Performance Fibre Reinforced Concrete (UHPFRC). Cem Concr Res 2014;56:29–39.
[26] Yu R, Tang P, Spiesz P, Brouwers HJH. A study of multiple effects of nano-silica and hybrid fibres on the properties of Ultra-High Performance Fibre Reinforced Concrete (UHPFRC) incorporating waste bottom ash (WBA). Constr Build Mater 2014;60:98–110.
[27] Yu R, Spiesz P, Brouwers HJH. Effect of nano-silica on the hydration and microstructure development of Ultra-High Performance Concrete (UHPC) with a low binder amount. Constr Build Mater 2014;65:140–50.
[28] Yu R, Spiesz P, Brouwers HJH. Static properties and impact resistance of a green Ultra-High Performance Hybrid Fibre Reinforced Concrete (UHPHFRC): experiments and modeling. Constr Build Mater 2014;68:158–71.
[29] Kim DJ, Park SH, Ryu GS, Koh KT. Comparative flexural behavior of Hybrid Ultra-High Performance Fiber Reinforced Concrete with different macro fibers. Constr Build Mater 2011;25:4144–55.
[30] Habel K, Viviani M, Denarié E, Brühwiler E. Development of the mechanical properties of an Ultra-High Performance Fiber Reinforced Concrete (UHPFRC). Cem Concr Res 2006;36(7):1362–70.
[31] Alberti MG, Enfedaque A, Gálvez JC, Cánovas MF, Osorio IR. Polyolefin fiber-reinforced concrete enhanced with steel-hooked fibers in low proportions. Mater Des 2014;60:57–65.
[32] Sebaibi N, Benzerzour M, Abriak NE. Influence of the distribution and orientation of fibres in a reinforced concrete with waste fibres and powders. Constr Build Mater 2014;65(29):254–63.
[33] Deeb R, Karihaloo BL, Kulasegaram S. Reorientation of short steel fibres during the flow of self-compacting concrete mix and determination of the fibre orientation factor. Cem Concr Res 2014;56:112–20.
[34] Shah AA, Ribakov Y. Recent trends in steel fibered high-strength concrete. Mater Des 2011;32(8–9):4122–51.
[35] Vincent T, Ozbakkaloglu T. Influence of fiber orientation and specimen end condition on axial compressive behavior of FRP-confined. Constr Build Mater 2013;47:814–26.
[36] Banthia N, Majdzadeh F, Wu J, Bindiganavile V. Fiber synergy in hybrid fiber reinforced concrete (HyFRC) in flexure and direct shear. Cem Concr Compos 2014;48:91–7.
[37] Ganesan N, Indira PV, Sabeena MV. Bond stress slip response of bars embedded in hybrid fibre reinforced high performance concrete. Constr Build Mater 2014;50:108–15.
[38] Yap SP, Bu CH, Alengaram UJ, Mo KH, Jumaat MZ. Flexural toughness characteristics of steel–polypropylene hybrid fibre-reinforced oil palm shell concrete. Mater Des 2014;57:652–9.
[39] Banthia N, Gupta R. Hybrid fiber reinforced concrete (HyFRC): fiber synergy in high strength matrices. Mater Struct 2004;37(10):707–16.
[40] Banthia N, Nandakumar N. Crack growth resistance of hybrid fiber reinforced cement composites. Cem Concr Compos 2003;25(1):3–9.
[41] Grünewald S. Performance-based design of self-compacting fibre reinforced concrete. Delft, The Netherlands: Delft University of Technology; 2004.
[42] Markovic I, High-performance hybrid-fibre concrete – development and utilisation [Ph.D. thesis]. Technische Universität Delft; 2006.
[43] Yao W, Li J, Wu K. Mechanical properties of hybrid fiber-reinforced concrete at low fiber volume fraction. Cem Concr Res 2003;33(1):27–30.
[44] Park SH, Kim DJ, Ryu GS, Koh KT. Tensile behaviour of Ultra-High Performance Hybrid Fibre Reinforced Concrete. Cem Concr Compos 2012;34:172–84.
[45] Rossi P, Acker P, Malier Y. Effect of steel fibres at two stages: the material and the structure. Mater Struct 1987;20:436–9.
[46] Ghafari E, Costa H, Júlio E. RSM-based model to predict the performance of self-compacting UHPC reinforced with hybrid steel micro-fibers. Constr Build Mater 2014;66(15):375–83.
[47] Tabatabaei ZS, Volz JS, Keener DI, Gliha BP. Comparative impact behavior of four long carbon fiber reinforced concretes. Mater Des 2014;55:212–23.
[48] Lin XS, Zhang YX, Hazell PJ. Modelling the response of reinforced concrete panels under blast loading. Mater Des 2014;56:620–8.
[49] Yi NH, Kim JHJ, Han TS, Cho YG, Lee JH. Blast-resistant characteristics of ultra-high strength concrete and reactive powder concrete. Constr Build Mater 2012;28:694–707.
[50] Su H, Xu J, Ren W. Mechanical properties of ceramic fiber-reinforced concrete under quasi-static and dynamic compression. Mater Des 2014;57:426–34.
[51] Wang S, Zhang M, Quek S. Mechanical behavior of fiber-reinforced high-strength concrete subjected to high strain-rate compressive loading. Constr Build Mater 2012;31:1–11.
[52] Funk JE, Dinger DR. Predictive process control of crowded particulate suspensions, applied to ceramic manufacturing. Boston, The United States: Kluwer Academic Publishers; 1994.
[53] Yu QL, Spiesz P, Brouwers HJH. Development of cement-based lightweight composites – Part 1: mix design methodology and hardened properties. Cem Concr Compos 2013;44:17–29.
[54] Spiesz P, Yu QL, Brouwers HJH. Development of cement-based lightweight composites – Part 2: durability related properties. Cem Concr Compos 2013;44:30–40.
[55] Hüsken G, Brouwers HJH. A new mix design concept for each-moist concrete: a theoretical and experimental study. Cem Concr Res 2008;38:1249–59.
[56] Brouwers HJH, Radix HJ. Self compacting concrete: theoretical and experimental study. Cem Concr Res 2005;35:2116–36.
[57] Quercia G, Spiesz P, Hüsken G, Brouwers HJH. SCC modification by use of amorphous nano-silica. Cem Concr Compos 2014;45:69–81.
[58] Brouwers HJH. Particle-size distribution and packing fraction of geometric random packings. Phys. Rev. E 2006;74. 031309-1-031309-14.
[59] Hunger M., An integral design concept for ecological self-compacting concrete [Ph.D. thesis]. Eindhoven University of Technology, The Netherlands: Eindhoven; 2010.
[60] Hüsken G, A multifunctional design approach for sustainable concrete with application to concrete mass products [Ph.D. thesis]. Eindhoven, The Netherlands: Eindhoven University of Technology; 2010.
[61] BS-EN-1015-3. Methods of test for mortar for masonry – Part 3: determination of consistence of fresh mortar (by flow table). British Standards Institution-BSI and CEN European Committee for Standardization; 2007.
[62] BS-EN-12350-8. Testing fresh concrete - Part 8: self-compacting concrete - Slump-flow test. British Standards Institution-BSI and CEN European Committee for Standardization; 2010.
[63] BS-EN-196-1. Methods of testing cement – Part 1: determination of strength. British Standards Institution-BSI and CEN European Committee for Standardization; 2005.
[64] BS EN 12390-3. Testing hardened concrete Part 3: Compressive strength of test specimens. British Standards Institution-BSI and CEN European Committee for Standardization; 2009.
[65] BS EN 12390-5. Testing hardened concrete – Part 5: flexural strength of test specimens. British Standards Institution-BSI and CEN European Committee for Standardization; 2009.
[66] ASTM C 1018-97. Standard test methods for flexural toughness and first crack strength of fibre reinforced concrete. American Society for Testing and Materials (ASTM), 1998, 04(02): 506–513.
[67] JSCE Standard SF-4. Method of test for flexural strength and flexural toughness of fibre reinforced concrete. Japan Society of Civil Engineers (JSCE); 1984.
[68] The European Guideline for Self-Compacting Concrete – Specification, Production and Use. The European Project Group, 2005.
[69] Boulekbache B, Hamrat M, Chemrouk M, Amziane S. Flowability of fibre-reinforced concrete and its effect on the mechanical properties of the material. Constr Build Mater 2010;24:1664–71.
[70] Nataraja MC, Dhang N, Gupta AP. Toughness characterization of steel fibre reinforced concrete by JSCE approach. Cem Concr Res 2000;30:593–7.
[71] Sukontasukkul P. Toughness evaluation of steel and polypropylene fibre reinforced concrete beams under bending. Thammasat Int J Sci Technol 2004;9(3):35–41.